SOME DYNAMICS OF ACOUSTIC OSCILLATIONS WITH NONLINEAR COMBUSTION AND NOISE

V. S. Burnley[1], F. E. C. Culick[2]

[1]U. S. Air Force Phillips Laboratory; [2]California Institute of Technology

ABSTRACT: The results given in this paper constitute a continuation of progress with nonlinear analysis of coherent oscillations in combustion chambers. We are currently focusing attention on two general problems of nonlinear behavior important to practical applications: the conditions under which a linearly unstable system will execute stable periodic limit cycles; and the conditions under which a linearly stable system is unstable to a sufficiently large disturbance. The first of these is often called 'soft' excitation, or supercritical bifurcation; the second is called 'hard' excitation, 'triggering,' or subcritical bifurcation and is the focus of this paper. Previous works extending over more than a decade have established beyond serious doubt (although no formal proof exists) that nonlinear gasdynamics alone does not contain subcritical bifurcations. The present work has shown that nonlinear combustion alone also does not contain subcritical bifurcations, but the combination of nonlinear gasdynamics and combustion does. Some examples are given for simple models of nonlinear combustion of a solid propellant but the broad conclusion just mentioned is valid for any combustion system.

Although flows in combustors contain considerable noise, arising from several kinds of sources, there is sound basis for treating organized oscillations as distinct motions. That has been an essential assumption incorporated in virtually all treatments of combustion instabilities. However, certain characteristics of the organized or deterministic motions seem to have the nature of stochastic processes. For example, the amplitudes in limit cycles always exhibit a random character and even the occurrence of instabilities seems occasionally to possess some statistical features. Analysis of nonlinear coherent motions in the presence of stochastic sources is therefore an important part of the theory. We report here a few results of power spectral densities of acoustic amplitudes in the presence of a subcritical bifurcation associated with nonlinear combustion and gasdynamics.

NOMENCLATURE

Symbol	Description
$\bar{a}$	speed of sound
f	function defined with Eq. (1.2)
F_n	forcing function defined in Eqs. (1.5) and (1.6)
$\mathcal{F}'$	defined in Eq. (2.1)
$F(\boldsymbol{u})$	defined in Eq. (2.3)
h	function defined with Eq. (1.1)

k_n	wavenumber of n^{th} mode
$\dot{m}_{\text{pc}}$	pressure-dependent mass flux, Eq. (2.3)
$\hat{n}$	unit outward normal vector
p'	pressure fluctuation
$\mathcal{P}'$	defined in Eq. (2.1)
$r_n(t)$	magnitude of the time-dependent amplitude $\eta_n(t)$
R_{vc}	constant defined in Eq. (2.3)
s'	entropy fluctuation
$\boldsymbol{u}'$	velocity fluctuation
u_t	threshold velocity (Figures 2 and 3)
Greek Symbols	
α_n	linear growth rate of n^{th} mode
$\eta_n(t)$	time-dependent amplitude of n^{th} mode
ρ'	density fluctuation
θ_n	linear frequency shift of n^{th} mode
ϕ_n	phase of the time-dependent amplitude $\eta_n(t)$
$\psi_n(\boldsymbol{r})$	mode-shape of n^{th} mode
ω_n	frequency of n^{th} mode
$\boldsymbol{\Omega}'$	vorticity fluctuation
Subscripts	
$(\ )_a$	acoustic waves
$(\ )_s$	entropy waves
$(\ )_\Omega$	vorticity waves

1 INTRODUCTION

Coherent oscillations have been a constant problem in the design of combustion systems. There are two general types of oscillations which are commonly found in combustion chambers: spontaneous oscillations and pulsed oscillations. A spontaneous oscillation occurs when the system is linearly unstable. As a result, any perturbation of the system grows exponentially in time. Under the influence of nonlinear effects, the pressure field may reach a periodic motion, or limit cycle. This type of instability is also known as an intrinsic instability or a soft excitation. In the field of dynamical systems, the change of behavior from linearly stable to linearly unstable is called a supercritical bifurcation. The problem of linear instability has been widely treated and will not covered in this paper.

A pulsed oscillation, on the other hand, is a true nonlinear instability of a linearly stable system. Small perturbations in the pressure field decay exponentially to zero, while larger perturbations may lead to stable or unstable periodic motions. Common terminology used to describe this type of oscillation includes triggered instability, hard excitation, and subcritical bifurcation. In the field of combustion instabilities, Sirignano and Crocco[1,2] were the first to examine pulsed oscillations using the method of characteristics and the $n-\tau$ model for the combustion dynamics. However, the calculations were quite complex and restrictive approximations were required in order to obtain results. No assessment was made as to the consequences of using these approximations. For several reasons, then, it is impossible to determine the general applicability of these results. Moreover, it is not possible to determine whether or not the pulsed oscillations were stable or unstable. Zinn and his students.[3–7] also studied pulsed oscillations in liquid propellant rocket motors using many of the same approximations used by Sirignano and Crocco (notably

the combustion model). As a result, those investigations suffer from the same shortcomings as the earlier works.

In the current study, we are primarily interested in the conditions under which stable pulsed oscillations can occur. We base the analysis on an approximate formulation which was developed over two decades ago by Culick.[8] The formulation has been covered in many other works, so only a brief overview of the method is presented here; for more details, see, e.g., the review by Culick.[9] The numerical calculations consist in applying a continuative method such that the results are guaranteed to represent stable limit cycles.

In order to keep the analysis as general as possible, the formulation begins with the conservation equations for two-phase flow. These equations are then rewritten into an equivalent form for a single medium having the mass-averaged properties of the two phases. Subsequently, a wave equation for the pressure is developed, along with the corresponding boundary condition.

$$\nabla^2 p' - \frac{1}{\bar{a}^2}\frac{\partial^2 p'}{\partial t^2} = h \tag{1.1}$$

$$\hat{\boldsymbol{n}} \cdot \nabla p' = -f \tag{1.2}$$

The functions h and f are linear and nonlinear functions of the pressure and velocity perturbations. As an approximation, these perturbations are expanded as a synthesis of classical acoustic modes with time-varying amplitudes,

$$p'(\boldsymbol{r}, t) = \bar{p} \sum_{n=1}^{\infty} \eta_n(t) \psi_n(\boldsymbol{r}) \tag{1.3}$$

$$\boldsymbol{u}'(\boldsymbol{r}, t) = \sum_{n=1}^{\infty} \frac{\dot{\eta}_n(t)}{\bar{\gamma} k_n^2} \nabla \psi_n(\boldsymbol{r}) \tag{1.4}$$

where ψ_n is the mode shape and $\eta_n(t)$ is the time-dependent amplitude of the n^{th} classical acoustic mode. After substituting Eq. (1.3) in Eq. (1.1), the equations are spatially averaged, resulting in a system of ordinary differential equations describing the amplitudes of the acoustic modes.

$$\frac{d^2 \eta_n}{dt^2} + \omega_n^2 \eta_n = F_n \tag{1.5}$$

where $\omega_n = \bar{a} k_n$ and

$$F_n = -\frac{\bar{a}^2}{\bar{p} E_n^2} \left\{ \int \psi_n h dV + \oint \psi_n f dS \right\} \tag{1.6}$$

Thus, the problem is reduced to solving for the amplitudes, $\eta_n(t)$. This approach is very general and can accommodate all damping and amplification mechanisms. The most difficult part of the problem is in the identification and modeling of the important physical processes.

Much of the earlier work using this analysis has concentrated on the effects of nonlinear contributions from gasdynamics only. Some of these include Yang et al.,[10] Paparizos and Culick,[11] and Jahnke and Culick.[12] These works have convincingly shown that nonlinear gasdynamics alone does not contain the possibility of pulsed oscillations. It has also been shown that results for nonlinear gasdynamics to second-order is qualitatively similar to results obtained using gasdynamics to third-order; we will therefore include nonlinear gasdynamics to second-order only. In this work, we will present results for systems with additional contributions from nonlinear combustion response and noise.

2 NONLINEAR COMBUSTION RESPONSE OF SOLID PROPELLANTS

Combustion of a solid propellant is nonlinear chiefly for two reasons: chemical processes depend nonlinearly on both temperature and pressure; and the conversion of condensed material to gaseous products is a nonlinear function of the properties of the local flow field. In the past, analysis of unsteady burning has been directed largely to investigating the response of burning to small fluctuations of the flow field in order to satisfy the need to predict linear stability. In particular, the response of burning to fluctuations in pressure has received the most attention; see Culick[13] for a review of calculations of the linear response function. In this section, we will show results for models of the nonlinear response of solid propellants.

In order to be used in the present analysis, any model of unsteady combustion must be put in such a form as to fit into the appropriate terms in the forcing function given by Eq. (1.6). For gasdynamics up to second-order, the right-hand side of Eq. (1.5) can be written:

$$-\frac{\bar{p}E_n^2}{a^2}F_n = \bar{\rho}\int(\bar{\boldsymbol{u}}\cdot\nabla\boldsymbol{u}' + \boldsymbol{u}'\cdot\nabla\bar{\boldsymbol{u}})\cdot\nabla\psi_n dV + \frac{1}{a^2}\frac{\partial}{\partial t}\int(\bar{\gamma}p'\nabla\cdot\bar{\boldsymbol{u}} + \bar{\boldsymbol{u}}\cdot\nabla p')\psi_n dV$$

linear gasdynamics

$$+\bar{\rho}\int\left[\boldsymbol{u}'\cdot\nabla\boldsymbol{u}' + \frac{\rho'}{\bar{\rho}}\frac{\partial\boldsymbol{u}'}{\partial t}\right]\cdot\nabla\psi_n dV + \frac{1}{a^2}\frac{\partial}{\partial t}\int(\bar{\gamma}p'\nabla\cdot\boldsymbol{u}' + \boldsymbol{u}'\cdot\nabla p')\psi_n dV \qquad (2.1)$$

nonlinear gasdynamics

$$+\oint\bar{\rho}\frac{\partial\boldsymbol{u}'}{\partial t}\cdot\hat{\boldsymbol{n}}\psi_n dS - \int\left[\frac{1}{a^2}\frac{\partial\mathcal{P}'}{\partial t}\psi_n + \boldsymbol{\mathcal{F}}'\cdot\nabla\psi_n\right]dV$$

linear and nonlinear surface processes — other contributions

As a means of accommodating nonlinear combustion of solid propellants, we are concerned with the term labeled "linear and nonlinear surface processes." Because this term is nearly equal to the time derivative of the second-order fluctuation of mass flux inward, it provides a means through which contributions from nonlinear combustion may be included. The mass flux at the surface is defined as $\dot{\boldsymbol{m}} = \rho\boldsymbol{u}$ so that the fluctuating part becomes

$$\begin{aligned}\dot{\boldsymbol{m}}' &= \dot{\boldsymbol{m}} - \bar{\dot{\boldsymbol{m}}}\\ &= (\bar{\rho}+\rho')(\bar{\boldsymbol{u}}+\boldsymbol{u}') - \bar{\rho}\bar{\boldsymbol{u}}\\ &= \bar{\rho}\boldsymbol{u}' + \rho'(\bar{\boldsymbol{u}}+\boldsymbol{u}')\end{aligned}$$

Assuming $\bar{\boldsymbol{u}}$ is independent of time, a form which can be directly substituted in Eq. (2.1) is obtained by taking the time derivative of the above equation and rearranging terms.

$$\bar{\rho}\frac{\partial\boldsymbol{u}'}{\partial t}\cdot\hat{\boldsymbol{n}} = \frac{\partial\dot{\boldsymbol{m}}'}{\partial t}\cdot\hat{\boldsymbol{n}} - \rho'\frac{\partial\boldsymbol{u}'}{\partial t}\cdot\hat{\boldsymbol{n}} - \frac{\partial\rho'}{\partial t}(\bar{\boldsymbol{u}}+\boldsymbol{u}')\cdot\hat{\boldsymbol{n}} \qquad (2.2)$$

It happens that analysis and modeling of unsteady combustion leads to results for mass fluctuation, but as shown by Eq. (2.1), the gasdynamics problem within the chamber requires the

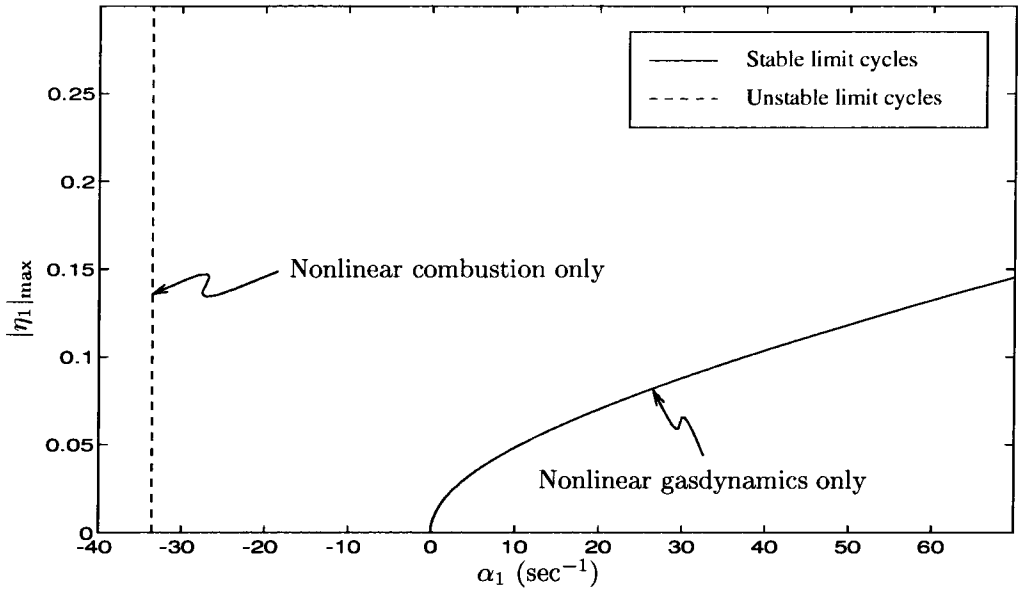

Figure 1. Maximum amplitude in limit cycle of first acoustic mode showing contributions of nonlinear gasdynamics and combustion

unsteady velocity as the boundary condition. Thus, we can include contributions from nonlinear combustion by use of Eq. (2.2).

For the results here, we assume that all linear processes are accounted for and that nonlinear contributions arise only from gasdynamics and/or combustion. When only nonlinear gasdynamics is included in the analysis, a supercritical bifurcation, characteristic of spontaneous oscillations, is produced; see Fig. 1. The basic input data for Figs. 1, 3 and 4 are those used by Culick and Yang[14] except for the special values needed in the representation of the nonlinear combustion response.

When combustion provides the only nonlinear contributions, the possibility of pulsed oscillations has also not been found. For the nonlinear combustion model used in Fig. 1, described in the following section, a shifted stability boundary was produced. No stable limit cycles are found on either side of this boundary. Other models of nonlinear combustion have produced similar results. Therefore, we have subsequently investigated the combination of nonlinear gasdynamics and combustion, and some of those results will be reproduced here.

Most of the work concerning combustion instabilities has dealt with linear stability of pressure oscillations. As a result, many models of the linear response of combustion to pressure oscillations have been developed.[15] In order to study the possible influences of nonlinear pressure coupling, one of these linear response functions was extended by retaining terms to second-order.[16] For reasonable values of parameters, this model did not produce triggering to stable limit cycles and will not be covered here; see Burnley[17] for details. Instead, we will concentrate on the response of combustion to velocity oscillations parallel to the burning surface, i.e., velocity coupling.

2.1 Velocity Coupling

In the experimental and theoretical investigation of pulsed instabilities by the Air Force Propulsion Laboratory, Baum and Levine[18] introduced a model of nonlinear combustion response based on the idea of velocity coupling. To obtain agreement between predicted behavior and observations, one parameter representing the response of combustion to the velocity parallel to the

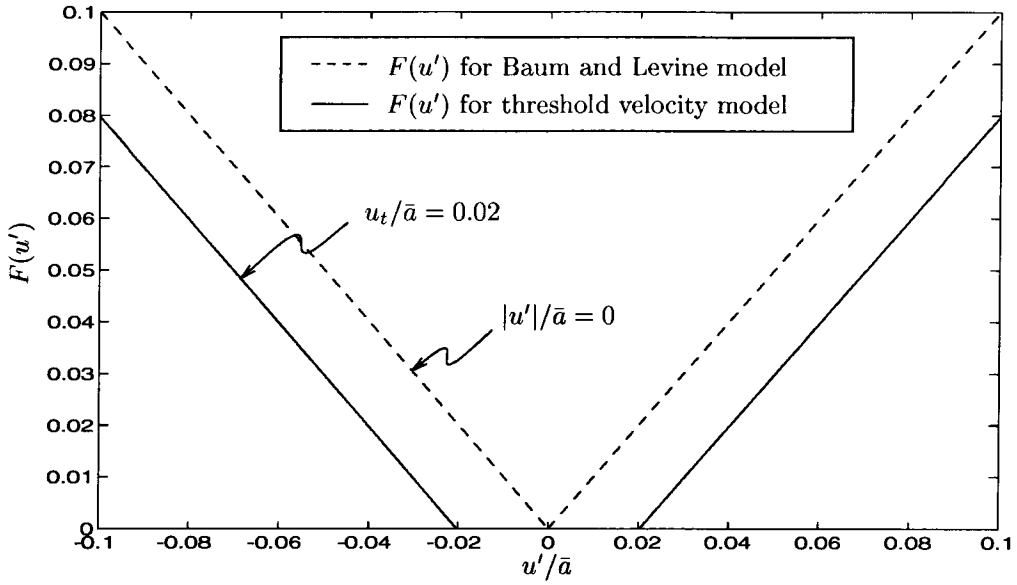

Figure 2. Function of velocity to be used in the threshold velocity model; $u_t/\bar{a} = 0.02$

burning surface was changed. By changing only this parameter, they were able to match the growth rates, the limit cycle amplitudes, the mean pressure shift, and the waveform quite accurately. This suggests that the chosen nonlinearity must be fairly close to the important physical processes present in the experiments.

The Baum and Levine model is an ad hoc model in which the mass burning rate is directly modified by some function of the velocity.[18] For that reason it was originally called the 'burn rate augmentation model.' The total mass burning rate is written as a combination of linear pressure coupling and nonlinear velocity coupling.

$$\dot{m} = \dot{m}_{\rm pc}[1 + R_{\rm vc}F(\boldsymbol{u})] \tag{2.3}$$

where $\dot{m}_{\rm pc}$ is the mass flux due to pressure only and $R_{\rm vc}$ is a constant related to the sensitivity of burning to velocity parallel to the surface. As the evolution rate of solid to gas should depend on the magnitude but not the direction of the scouring flow, and the simplest assumption is linear dependence, $F(\boldsymbol{u})$ is taken equal to $|\boldsymbol{u}'|/\bar{a}$. We will restrict $R_{\rm vc}$ to positive values, i.e., cases in which the mass flux decreases due to velocity fluctuations will not be considered.

A second model which will be discussed in this section is based on the idea of a threshold velocity. Threshold effects have been observed in experimental investigations of velocity coupling. Ma et al.[19] used subliming dry ice to simulate the flow in a solid propellant rocket motor. A piston was used to generate acoustic waves in the chamber. The investigation found a threshold acoustic velocity above which the mean mass flux increased linearly with the Reynolds number of the acoustic fluctuations. Below the threshold value, the mean mass flow was approximately constant. The increased mass flux was determined to be a result of increased heat transfer to the surface after transition to turbulent flow had occurred.

The function of velocity shown in Figure 2 will be used in the Baum and Levine model (2.3) to construct the threshold velocity model. This function introduces a dead zone in which the nonlinear contributions from combustion do not affect the system. When the amplitudes of oscillations become larger than the chosen threshold value u_t, the nonlinear effects are then felt.

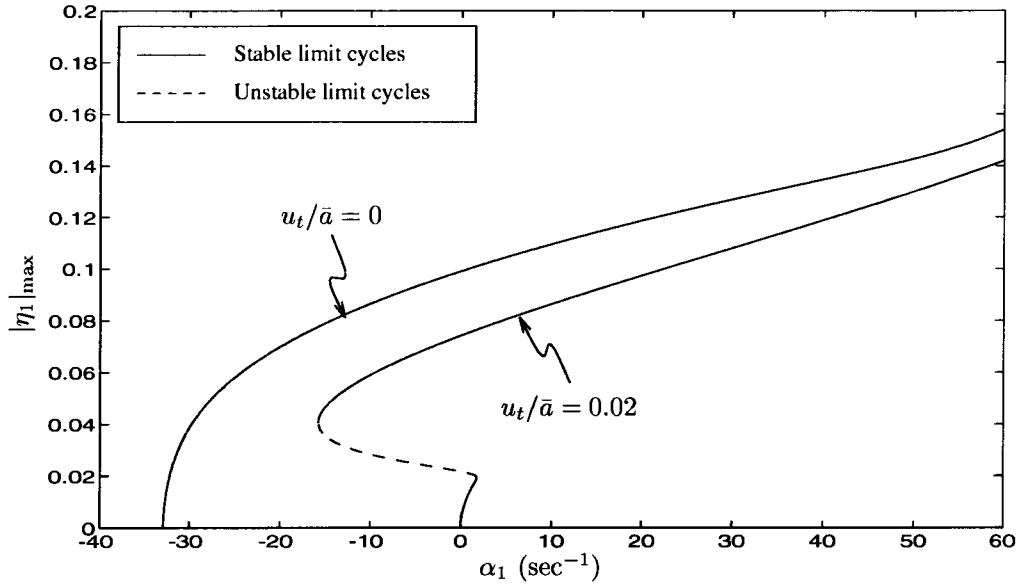

Figure 3. Maximum amplitude in limit cycle of first acoustic mode with and without a normalized threshold velocity of 0.02; four modes; $R_{vc} = 5.32$

2.1.1 Results for velocity coupling

The Baum and Levine model as originally formulated did not satisfactorily explain pulsed oscillations. Although regions of possible triggering were found when the system was truncated to two modes, this region is greatly reduced or is no longer present when more modes are included. The threshold velocity model, on the other hand, produces sizeable regions of possible triggering. In Fig. 3, results for the Baum and Levine model is compared with results for a normalized threshold velocity $(u_t/\bar{a})$ of 0.02.

For velocity oscillations with amplitudes less than the chosen threshold velocity, the effect of nonlinear combustion is nonexistent. Therefore, the path of periodic solutions should be identical to the case of linear pressure coupling, i.e., a supercritical bifurcation occurring at the origin. This is precisely the behavior shown in Fig. 3 for the threshold velocity model. Once the magnitude of the velocity oscillations reaches the threshold value, nonlinear combustion quickly

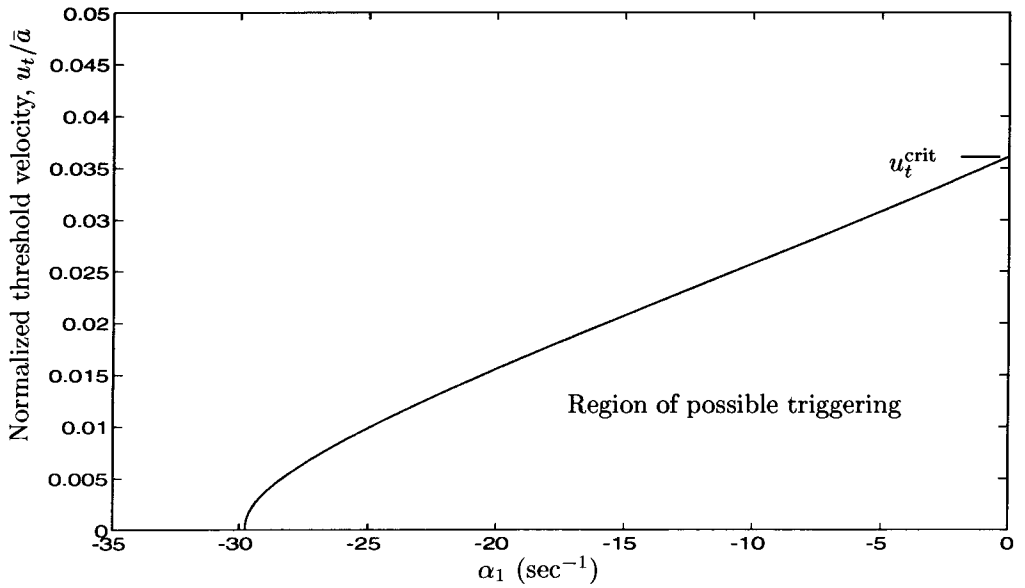

Figure 4. Influence of the threshold velocity u_t on the region of possible triggering; $R_{vc} = 5.32$

becomes important, and a fold in the path is produced. The unstable path remains nearly horizontal until other nonlinear contributions become strong enough to produce a second fold, thereby producing a path of stable periodic solutions. Another observation from Fig. 3 is that the amplitudes of oscillations are lower than the amplitudes for a zero threshold velocity. The total energy provided by nonlinear combustion during one cycle is less when a threshold velocity is present. Thus, lower amplitudes are required in order to dissipate the energy and maintain a stable limit cycle.

Using the methods of dynamical systems theory, the location of the upper turning point was determined as a function of the threshold velocity. For a value of $R_{vc} = 5.32$, a plot of this dependence is provided in Fig. 4. (Note that there is a discrepancy between Figs. 3 and 4 for $u_t/\bar{a} = 0$. This is due to the quantitative inaccuracy of the original oscillator equations when using the threshold velocity model in the methods of dynamical systems theory; see Burnley[17] for details. The plot of $u_t/\bar{a} = 0$ in Fig. 3 was generated using time-averaged equations, while Fig. 4 was produced using the original oscillator equations. For $u_t/\bar{a} \approx 0$, the time-averaged equations are slightly more accurate than the original oscillator equations.) There is actually no triggering for $u_t/\bar{a} = 0$, although a large region of possible triggering exists for $u_t/\bar{a}$ infinitesimally greater than zero. As u_t is increased, the region becomes increasingly smaller until finally, a critical value is reached above which triggering is no longer possible. This phenomenon was noted by Levine and Baum,[18] but no possible explanations were given.

If the threshold velocity is greater than u_t^{crit}, the rate of energy production by nonlinear combustion cannot equal the rate at which energy is transferred to higher modes by nonlinear gasdynamics. Therefore, for a stable limit cycle to exist, additional energy must be provided by linear processes, i.e., $\alpha_1 > 0$. For this reason, a propellant with a very high threshold velocity will be impossible to trigger. It was also determined that the critical value of u_t depends directly on the value of the velocity coupled response function, as one would expect. The rate of energy production is proportional to R_{vc}. As the coupling to velocity oscillations becomes stronger, i.e., R_{vc} increases, u_t^{crit} increases accordingly.

3 THE INFLUENCE OF COMBUSTION NOISE

Combustion chambers are inherently noisy environments. This is apparent from inspection of the power spectra of pressure records from test firings, as well as from simply listening to the test. When a combustion instability is present, the power spectrum exhibits well-defined peaks in addition to background noise over the entire range of frequencies. Substantial noise sources in rocket motors include flow separation, turbulence, and combustion processes. It is expected that the presence of noise will affect in some way the amplitudes and possibly the qualitative behavior of coherent oscillations. That is precisely the purpose of this section: to determine the influence of noise on combustion instabilities.

Only a small amount of work has been done on the interactions between noise and acoustic instabilities. Culick et al.[20] studied the influence of noise on combustion instabilities, but only for a very simple case: two acoustic modes with noise present only in the first mode. In addition, the formulation was flawed, and the form of the resulting noise terms is not quite correct. Clavin et al.[21] studied the influence of turbulence on instabilities in liquid rocket motors. Using only one mode in the analysis and third-order nonlinearities, it was reported that the inclusion of noise can lead to the possibility of triggering. It is a well-known result that a single third-order equation may produce a subcritical bifurcation. When more acoustic modes are considered, this may not be the case, as demonstrated by Yang et al.[10] for third-order gasdynamics. Therefore, the results of Clavin et al. may not be applicable in general.

The present analysis is an extension of the previous work by Culick et al.[20] We will first decompose the flow field into acoustic and non-acoustic parts using a method developed by Chu and Kovásznay.[22] This will allow the general form of the noise terms to be determined. Finally, we will simplify the equations in order to study the possible influences of noise on combustion instabilities.

3.1 Splitting the Unsteady Flow Field Into Acoustic, Vortical, and Entropic Modes of Propagation

Fluctuations in a compressible fluid can be decomposed into three types of waves: acoustic waves, vorticity waves, and entropy waves. A thorough discussion of this idea is presented by Chu and Kovásznay.[22] The three waves propagate independently in linearized theory of a uniform mean flow, but are coupled when the mean flow is non-uniform.[23] For example, the pressure in an acoustic wave is changed slightly by the presence of a vorticity or entropy wave if the mean flow is not uniform. Coupling between modes may also occur at the boundaries of the chamber.

Although noise is detected as pressure waves, the *sources* of noise are associated with the presence of vorticity fluctuations (e.g., turbulence, flow separation, etc.) and entropy or non-isentropic temperature fluctuations. Therefore, decomposing the unsteady flow field into the three types of waves allows both noise and acoustic instabilities to be handled in the same analytical framework discussed in Sec. 1. The contributions from vorticity and entropy waves will appear as additional force terms on the right-hand side of the acoustic equation.

Following the analysis of Chu and Kovásznay,[22] the thermodynamic and kinematic variables can be written as a sum of fluctuations in the three waves as follows.

$$p' = p'_a + p'_\Omega + p'_s \tag{3.1}$$
$$\boldsymbol{\Omega}' = \boldsymbol{\Omega}'_a + \boldsymbol{\Omega}'_\Omega + \boldsymbol{\Omega}'_s \tag{3.2}$$
$$s' = s'_a + s'_\Omega + s'_s \tag{3.3}$$
$$\boldsymbol{u}' = \boldsymbol{u}'_a + \boldsymbol{u}'_\Omega + \boldsymbol{u}'_s \tag{3.4}$$

In general, all of the fluctuations will be nonzero, but not all terms are the same order. If we restrict the analysis to small amplitude motions, the three waves have the following characteristics:[22]

$(\,)_a$ acoustic waves: pressure and velocity fluctuations, no entropy change
$(\,)_\Omega$ vorticity waves: velocity fluctuations, no pressure or entropy changes
$(\,)_s$ entropy waves: entropy and velocity fluctuations, no pressure change

Thus, to zeroth-order, the fluctuations in the three waves are given by

$$p' = p'_a \tag{3.5}$$
$$\boldsymbol{\Omega}' = \boldsymbol{\Omega}'_\Omega \tag{3.6}$$
$$s' = s'_s \tag{3.7}$$
$$\boldsymbol{u}' = \boldsymbol{u}'_a + \boldsymbol{u}'_\Omega + \boldsymbol{u}'_s \tag{3.8}$$

An equation for the density fluctuation is obtained by expanding the formula for the entropy of a perfect gas.

$$\frac{\rho'}{\bar{\rho}} = \frac{1}{\bar{\gamma}}\frac{p'_a}{\bar{p}} - \frac{1}{\bar{c}_p}s' \tag{3.9}$$

As an approximation to the acoustic pressure and velocity perturbations, we will once again use a superposition of the classical acoustic modes so that

$$p'_a = \bar{p}\sum_{n=1}^{\infty}\eta_n(t)\psi_n(\boldsymbol{r}) \qquad \boldsymbol{u}'_a = \sum_{n=1}^{\infty}\frac{\dot{\eta}_n(t)}{\bar{\gamma}k_n^2}\nabla\psi_n(\boldsymbol{r})$$

Substitution of Eq. (3.5) in the left-hand side of the nonlinear wave equation (1.1), followed by application of Galerkin's method, leads to a set of coupled nonlinear oscillator equations.

$$\ddot{\eta}_n + \omega_n^2\eta_n = F_n \tag{3.10}$$

The right-hand side will be slightly different from the previous derivation with F_n given by:[23]

$$-\frac{\bar{p}E_n^2}{\bar{a}^2}F_n = \bar{\rho}I_1 + \frac{1}{\bar{a}^2}I_2 + \bar{\rho}I_3 + \frac{1}{\bar{a}^2}I_4 + \int\bar{\rho}\frac{\partial\boldsymbol{u}'}{\partial t}\cdot\hat{\boldsymbol{n}}dS - \int\left[\frac{1}{\bar{a}^2}\frac{\partial\mathcal{P}'}{\partial t}\psi_n + \boldsymbol{\mathcal{F}}'\cdot\nabla\psi_n\right]dV \tag{3.11}$$

where

$$I_1 = \int(\bar{\boldsymbol{u}}\cdot\nabla\boldsymbol{u}' + \boldsymbol{u}'\cdot\nabla\bar{\boldsymbol{u}})\cdot\nabla\psi_n dV \qquad I_2 = \frac{\partial}{\partial t}\int(\bar{\gamma}p'\nabla\cdot\bar{\boldsymbol{u}} + \bar{\boldsymbol{u}}\nabla\cdot p')\psi_n dV$$

$$I_3 = \int\left(\boldsymbol{u}'\cdot\nabla\boldsymbol{u}' + \frac{\rho'}{\bar{\rho}}\frac{\partial\boldsymbol{u}'}{\partial t}\right)\cdot\nabla\psi_n dV \qquad I_4 = \frac{\partial}{\partial t}\int(\bar{\gamma}p'\nabla\cdot\boldsymbol{u}' + \boldsymbol{u}'\cdot\nabla p')\psi_n dV$$

In the original development of the approximate analysis, the zeroth-order approximations for the pressure and velocity were used to evaluate F_n. The same idea will be applied here, although additional contributions to the velocity fluctuation from coupling to vorticity and entropy waves will be included. Once these quantities are substituted in the right-hand side, the set of forced oscillator equations eventually takes the general form

$$\ddot{\eta}_n + \omega_n^2\eta_n = 2\alpha_n\dot{\eta}_n + 2\omega_n\theta_n\eta_n - \sum_{i=1}^{\infty}\sum_{j=1}^{\infty}[A_{nij}\dot{\eta}_i\dot{\eta}_j + B_{nij}\eta_i\eta_j] + (F_n)_{\text{other}}^{\text{NL}} + \sum_{i=1}^{\infty}[\xi_{ni}^v\dot{\eta}_i + \xi_{ni}\eta_i] + \Xi_n \tag{3.12}$$

This system of equations is very complex, and there are many free parameters. For instance, if we truncate the system to N modes, there are $2N$ linear parameters and an additional $2N^2+N$ unknown functions. In order to simplify the equations somewhat, we will therefore neglect cross-coupling terms in ξ_{ni}^v and ξ_{ni}, i.e., terms with $n \neq i$. These terms may turn out to be important, but neglecting them will allow for easier initial computation of results and will suffice for the purposes here. The simplified set of equations is

$$\ddot{\eta}_n + \omega_n^2\eta_n = 2\alpha_n\dot{\eta}_n + 2\omega_n\theta_n\eta_n - \sum_{i=1}^{\infty}\sum_{j=1}^{\infty}[A_{nij}\dot{\eta}_i\dot{\eta}_j + B_{nij}\eta_i\eta_j] + (F_n)_{\text{other}}^{\text{NL}} + \xi_n^v(t)\dot{\eta}_n + \xi_n(t)\eta_n + \Xi_n(t) \tag{3.13}$$

3.2 Modeling of the Stochastic Sources

The problem has now been reduced to solving Eq. (3.13) for the time-dependent amplitudes $\eta_n(t)$ which are subjected to additive and multiplicative white noise. The source terms $\xi_n^v(t)$, $\xi_n(t)$, and $\Xi_n(t)$ represent stochastic processes of some sort and are responsible, in this formulation,

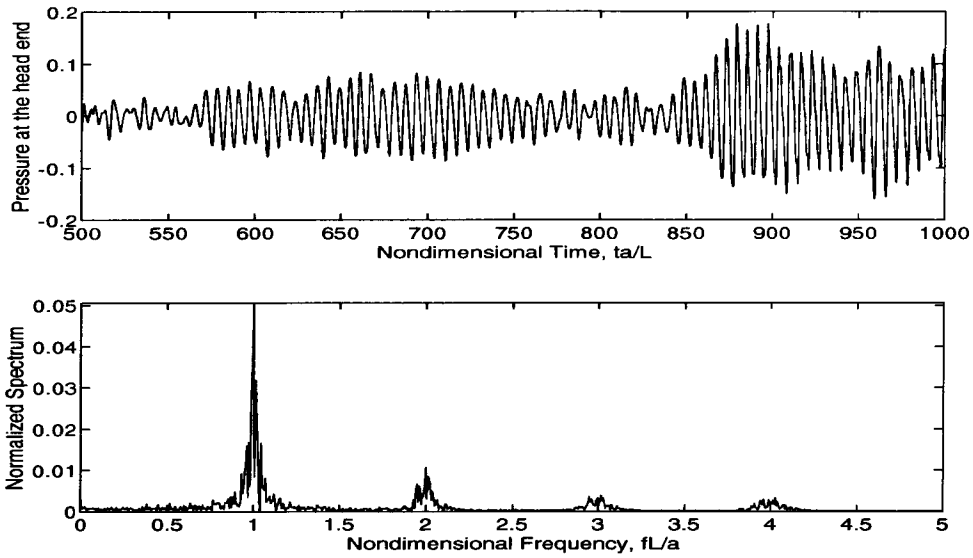

Figure 5. Sample pressure trace and spectrum for a simulation

for the background noise found in the power spectra of test firings. The problem of modeling these processes, however, remains. This requires specification of both the spatial and temporal distribution of the velocity and the entropy. At the present time, no models exist for these fluctuations.

There are several other paths that can be followed at this point which include obtaining approximate representations for the velocity and entropy fluctuations based on experimental data or numerical simulations. The approach that will be taken here is to assume forms for the source terms which are based on observations of experiments. By inspection of the pressure traces of test firings, it is apparent that the stochastic processes in real systems are broadband with very small correlation times, tau_c. (The correlation time is the time above which the autocorrelation function is zero. This is a measure of the dependence of the process on its past.) The limit $\tau_c \to 0$ represents a delta correlated process, i.e., a process which is totally uncorrelated with itself. It is thus interesting to study this limiting case and assume that the stochastic terms are represented by *white noise.*

The definition of a white noise process is a process whose spectral density is flat, i.e., all frequencies are present at the same amplitude. Although such a process cannot occur in a real system, white noise can be a very useful tool for studying real processes which have very small correlation times compared to the macroscopic times of the system. This is true of the random processes and systems of interest.[20] Therefore, we will approximate ξ_n^v, ξ_n, and Ξ_n by mutually independent white noise processes with zero mean values and intensities $\sigma_n^{\xi^v}$, σ_n^{ξ}, and σ_n^{Ξ}.

An example of a simulation with white noise excitations is presented in Fig. 5. A sample pressure trace is shown along with the corresponding normalized spectrum. Inspection of the spectrum shows the distinct frequencies which are associated with an acoustic instability, along with broadband background noise. This is characteristic of actual test data of a case when an instability is present.

3.3 The Effects of Noise and Nonlinear Combustion

In Section 2, we were interested only in deterministic systems. Since we are now studying nondeterministic systems, it is natural to use the probability density functions of the amplitudes

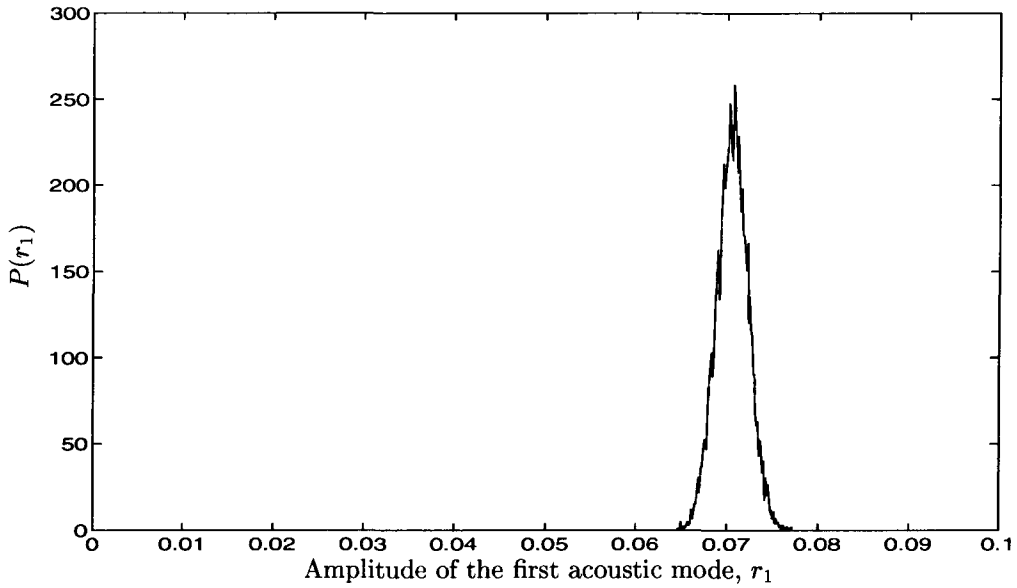

Figure 6. Probability density function for a system with a noisy linear growth rate in the fundamental mode only; 2 modes, $\sigma_1^{\xi^v} = 0.005$ sec$^{-3/2}$, $\alpha_1 = 25$ sec^{-1}

of acoustic modes to investigate the dynamics of the system. In addition, we will use the amplitude r_n which is defined in the following equation.

$$\eta_n(t) = r_n(t)\cos(\omega_n t + \phi_n(t)) \tag{3.14}$$

This amplitude will have a nonzero mean value so that quantitative changes will be more evident.

A Monte-Carlo method will be used to obtain an approximation to the probability density functions of the acoustic amplitudes. In this method, a series of numerical "experiments" is conducted, usually in the same manner that one would conduct actual experiments. After the flow field has become well-developed (say 1000 periods of the fundamental mode or so), the amplitudes of the acoustic modes are sampled. The results are then used to construct histograms which, after normalization, approximate the instantaneous probability density functions of the modal amplitudes. The approximation becomes better as the number of experiments is increased.

In the current study, each Monte-Carlo simulation will consist of 10000 numerical experiments. The linear parameters will be fixed throughout a series of experiments, while the initial conditions for the simulations will be varied systematically. In particular, a square initial pulse which is nonzero from $0 \leq x/L \leq .25$ will be used. The size of the pressure pulse $p'/\bar{p}$ will be varied from 0 to .2 linearly so as to include all likely values.

It is to be expected that the inclusion of combustion noise may well change the quantitative and perhaps even the qualitative behavior of solution. A previous investigation[17] was unable to find cases consistent with subcritical bifurcations when only nonlinear gasdynamics were included. All cases had only one apparent attractive state; see Fig. 6 for an example of a case with a noisy linear growth rate of the fundamental mode. As no examples of triggering were found for the case of noise and nonlinear gasdynamics, nonlinear combustion in the form of the threshold velocity model was also included in the analysis. The results are reproduced here.

When nonlinear combustion is added to the stochastic system (3.13), the resulting probability density functions can be quite different, as one might expect. We have previously shown in Section 2 that this model can produce regions of possible triggering in which two stable solutions exist simultaneously. In a stochastic system, this corresponds to a bimodal probability density

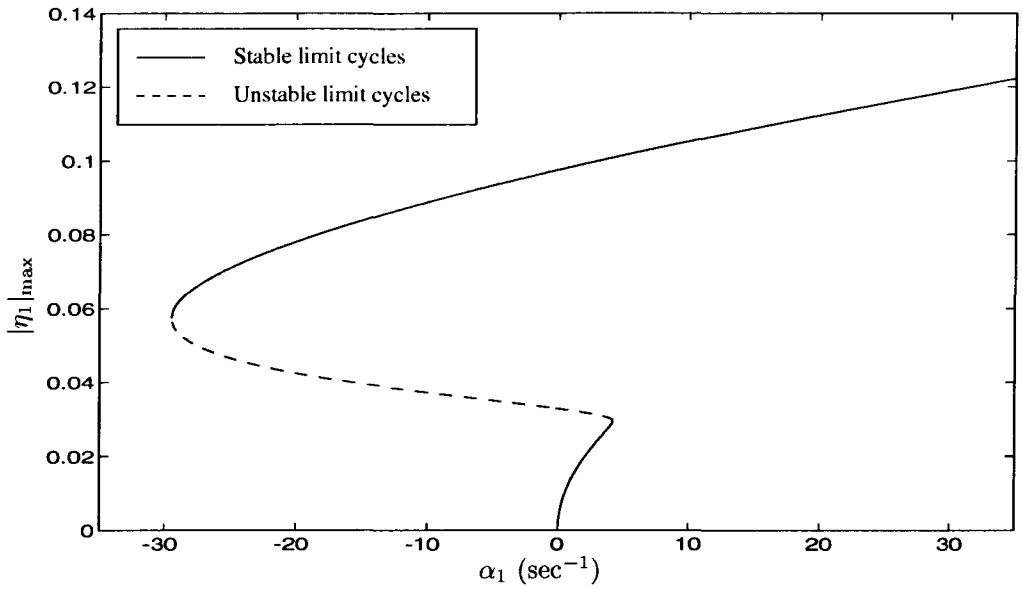

Figure 7. Bifurcation diagram for the deterministic system; threshold velocity model, $u_t/\bar{a} = 0.03$, $R_{vc} = 7.8$, 4 modes

function such that there is a high probability of low and high amplitudes and a low probability of intermediate values.

For the parametric values in the threshold velocity model, we will use $u_t/\bar{a} = 0.03$ and $\bar{R}_{vc} = 7.8$ for the parameters in the threshold velocity model. Using these values, the bifurcation diagram for the deterministic system is shown in Fig. 7. This diagram will be useful in the discussion of results. In addition, the following values were chosen for the intensities of the stochastic sources: $\sigma_n^{\xi^v} = 0.005$ sec$^{-3/2}$, $\sigma_n^{\xi} = 0.025$ sec$^{-1/2}$, and $\sigma_n^{\Xi} = 0.0005$ sec$^{-3/2}$, for $n = 1, 2$. The parameter α_1 will be varied while all other parametric values remain fixed. By changing this parameter, we will demonstrate a variety of the possible forms of the probability density functions.

From inspection of Fig. 7, we see that the region of possible triggering begins at approximately $\alpha_1 = -30$ sec^{-1} for the deterministic system. Below this value, the deterministic system is stable to any size perturbation. To illustrate the effect of noise on such a system, a linear growth rate of -35 sec^{-1} was chosen. Figure 8a shows the resulting probability density function for the first acoustic mode. For this case, the attractor of the deterministic system, i.e., the trivial steady state, is so strong that the amplitudes never reach large values. Therefore, the parametric excitations, i.e., ξ_n^{ν} and ξ_n, have a very small effect on the system. Most of the noise contribution is a result of the external excitations, Ξ_n.

As the linear growth rate is increased to a value above -30 sec^{-1}, we enter the region of possible triggering where an additional attractive state is present. Three values of α_1 were chosen in order to show how the probability density of the fundamental mode changes throughout this region. As the value of α_1 is varied, the regions of attraction of the stationary states will change. This will have a noticeable effect on the probability density functions.

The first value of α_1 was chosen very close to the lower boundary of the region of possible triggering. For a value of $\alpha_1 = -25$ sec^{-1}, Figure 8b shows the probability density function of the fundamental mode. The low amplitude attractive state is dominant because the region of attraction for this state is larger. However, the effect of the high amplitude attractive state is still present, resulting in a long tail in the probability density function.

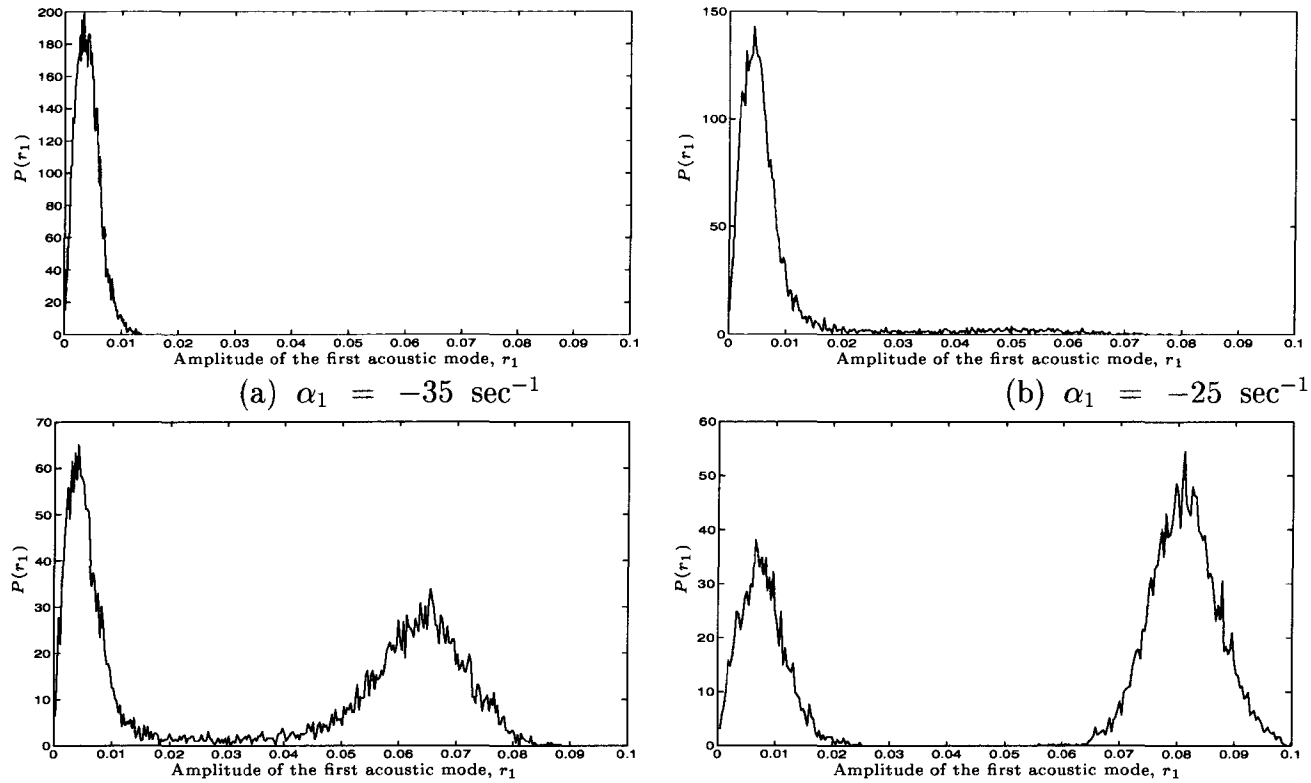

(a) $\alpha_1 = -35$ sec^{-1} (b) $\alpha_1 = -25$ sec^{-1}

(c) $\alpha_1 = -20$ sec^{-1} (d) $\alpha_1 = -10$ sec^{-1}

Figure 8. Probability density function of the first acoustic mode for various values of α_1; threshold velocity model, $u_t/\bar{a} = 0.03$, $R_{vc} = 7.8$, 4 modes

As we increase α_1 further to a value of -20 sec^{-1}, the effect of the high amplitude state becomes more noticeable, as shown in Figure 8c. The regions of attraction of the two states are becoming more equal so that amplitudes surrounding both states have high probabilities. Note that the probability density function is continuous, and the intermediate values are nonzero. This means that the background noise can lead to a qualitative change in the behavior of the system. This is not consistent with the usual definition of triggering in which a larger amplitude perturbation is necessary.

Figure 8d corresponds to $\alpha_1 = -10$ sec^{-1}. This figure is a good example of triggering in the presence of noise. The background noise is generally insufficient to cause transition from the low amplitude state to the high amplitude state. However, since we are assuming Gaussian distributed noise, even large amplitude perturbations are possible, and the stationary probability density function will in fact be continuous. The probability of intermediate amplitudes will, nonetheless, be very small.

4 CONCLUDING REMARKS

In this paper, we have presented some recent results of a continuing investigation on coherent oscillations in combustion chambers. Past studies have established that nonlinear gasdynamics alone does not explain pulsed oscillations. Using several models of nonlinear combustion, we have shown that nonlinear combustion alone does not apparently contain subcritical bifurcations either. The combination of the two, however, can produce the type of coupling between combustion processes and acoustic oscillations necessary for this type of behavior to occur. We

have reproduced some results obtained using a model of velocity coupling with a threshold. This model, which is based on a physically observed phenomenon, is sufficient to explain pulsed oscillations.

Most past studies of acoustic oscillations have neglected vortical and entropic waves. (For important recent exceptions, see Flandro[24] and Roh et al.[25]) We have relaxed that assumption and developed the general form for the noise terms which arise from vorticity, etc. In order to determine if the combination of combustion noise and nonlinear gasdynamics is sufficient to produce pulsed oscillations, a systematic study was performed. No cases of bimodal probability density functions were located, and it appears that combustion noise alone cannot produce that type of behavior. When the threshold velocity model is also included in the analysis, bimodal probability density functions are possible, as demonstrated here.

REFERENCES

[1] **Sirignano, W. A.,** *A Theoretical Study of Nonlinear Combustion Instability: Longitudinal Mode*, Ph.D. thesis, Princeton Univ., Princeton, NJ, 1964.

[2] **Sirignano, W. A. and Crocco, L.,** "A Shock Wave Model of Unstable Rocket Combustors," *AIAA Journal*, Vol. 2, No. 7, pp. 1285–1296, 1964.

[3] **Zinn, B. T. and Powell, E. A.,** "Application of the Galerkin Method in the Solution of Combustion Instability Problems," *Proceedings of the 19th International Astronautical Congress*, Vol. 3, pp. 59–73, 1970.

[4] **Powell, E. A. and Zinn, B. T.,** "A Single Mode Approximation in the Solution of Nonlinear Combustion Instability Problems," *Combustion Science and Technology*, Vol. 3, pp. 121–132, 1971.

[5] **Powell, E. A., Padmanabhan, M. S., and Zinn, B. T.,** "Approximate Nonlinear Analysis of Solid Rocket Motors and T-Burners: Volume 1," Air Force Rocket Propulsion Laboratory, Technical Report AFRPL-TR-77-48, Edwards AFB, CA 93523, 1977.

[6] **Zinn, B. T. and Lores, E. M.,** "Application of the Galerkin Method in the Solution of Nonlinear Axial Combustion Instability Problems in Liquid Rockets," *Combustion Science and Technology*, Vol. 4, No. 6, pp. 269–278, 1972.

[7] **Lores, E. M. and Zinn, B. T.,** "Nonlinear Longitudinal Instability in Rocket Motors," *Combustion Science and Technology*, Vol. 7, No. 6, pp. 245–256, 1973.

[8] **Culick, F. E. C.,** "Nonlinear Growth and Limiting Amplitude of Acoustic Oscillations in Combustion Chambers," *Combustion Science and Technology*, Vol. 3, No. 1, pp. 1–16, 1971.

[9] **Culick, F. E. C.,** "Some Recent Results for Nonlinear Acoustics in Combustion Chambers," *AIAA Journal*, Vol. 32, No. 1, pp. 146–169, 1994.

[10] **Yang, V., Kim, S. I., and Culick, F. E. C.,** "Third-Order Nonlinear Acoustic Waves and Triggering of Pressure Oscillations in Combustion Chambers, Part I: Longitudinal Modes," in *AIAA 25th Aerospace Sciences Meeting*, AIAA Paper 87-1873, 1987.

[11] **Paparizos, L. and Culick, F. E. C.,** "The Two-Mode Approximation to Nonlinear Acoustics in Combustion Chambers. I. Exact Solutions for Second Order Acoustics," *Combustion Science and Technology*, Vol. 65, No. 5, pp. 39–65, 1989.

[12] **Jahnke, C. C. and Culick, F. E. C.,** "An Application of Dynamical Systems Theory to Nonlinear Combustion Instabilities," *Journal of Propulsion and Power*, Vol. 10, No. 4, pp. 508–517, 1994.

[13] **Culick, F. E. C.,** "A Review of Calculations of Unsteady Burning of a Solid Propellant," *AIAA Journal*, Vol. 6, No. 12, pp. 2241–2255, 1968.

[14] **Culick, F. E. C. and Yang, V.,** "Prediction of the Stability of Unsteady Motions in Solid Propellant Rocket Motors," Chapter 18 in *Nonsteady Burning and Combustion Stability of Solid Propellants*, Progress in Astronautics and Aeronautics, Vol. 143, p. 719, 1992.

[15] **Culick, F. E. C.,** "Some Problems in the Unsteady Burning of Solid Propellants," Naval Weapons Center, Research Report NWC TP 4668, China Lake, CA, 1969.

[16] **Burnley, V. S., Swenson, G., and Culick, F. E. C.,** "Pulsed Instabilities in Combustion Chambers," in *31st AIAA/ASME/SAE/ASEE Joint Propulsion Conference*, AIAA Paper 95-2430, 1995.

[17] **Burnley, V. S.,** *Nonlinear Combustion Instabilities and Stochastic Sources*, Ph.D. thesis, California Institute of Technology, 1996.

[18] **Levine, J. N. and Baum, J. D.,** "A Numerical Study of Nonlinear Instability Phenomena in Solid Rocket Motors," *AIAA Journal*, Vol. 21, No. 4, pp. 557–564, 1983.

[19] **Ma, Y., Moorhem, W. K. Van, and Shorthill, R. W.,** "Experimental Investigation of Velocity Coupling in Combustion Instability," *Journal of Propulsion and Power*, Vol. 7, No. 5, pp. 692–699, 1991.

[20] **Culick, F. E. C., Paparizos, L., Sterling, J., and Burnley, V.,** "Combustion Noise and Combustion Instabilities in Propulsion Systems," in *Proceedings of the AGARD Conference on Combat Aircraft Noise*, AGARD CP 512, 1992.

[21] **Clavin, P., Kim, J. S., and Williams, F. A.,** "Turbulence-Induced Noise Effects on High-Frequency Combustion Instabilities," *CST*, Vol. 96, pp. 61–84, 1994.

[22] **Chu, B.-T. and Kovásznay, L. S. G.,** "Nonlinear Interactions in a Viscous Heat-conducting Compressible Gas," *Journal of Fluid Mechanics*, Vol. 3, No. 5, pp. 494–514, 1958.

[23] **Culick, F. E. C.,** "Nonlinear Acoustics in Combustion Chambers With Stochastic Sources," Guggenheim Jet Propulsion Center, California Institute of Technology, Documents on Active Control of Combustion Instabilities CI95-6, 1995.

[24] **Flandro, G. A.,** "Effects of Vorticity on Rocket Combustion Stability," *Journal of Propulsion and Power*, Vol. 11, No. 4, pp. 607–625, 1995.

[25] **Roh, T.-S., Tseng, I.-S., and Yang, V.,** "Effects of Acoustic Oscillations in Flame Dynamics of Homogeneous Propellants in Rocket Motors," *Journal of Propulsion and Power*, Vol. 11, No. 4, pp. 640–650, 1995.